

Strained-Si modulation doped field effect transistors as detectors of terahertz and sub-terahertz radiation

S L Rumyantsev^{1,2}, K Fobelets³, D Veksler¹, T Hackbarth⁴ and M S Shur¹

¹ Department of Electrical, Computer, and Systems Engineering, CII 9017, Rensselaer Polytechnic Institute, Troy, NY 12180–3590, USA

² Ioffe Institute of Russian Academy of Sciences, 194021 St Petersburg, Russia

³ Department of Electrical and Electronic Engineering, Imperial College London, Exhibition Road, London SW7 2BT, UK

⁴ DaimlerChrysler Research Center, Wilhem-Runge Strasse 11, 89081 Ulm, Germany

Received 12 May 2008

Published 28 August 2008

Online at stacks.iop.org/SST/23/105001

Abstract

Strained-Si modulation doped field effect transistors have been studied as detectors of 0.2 THz and 1.6 THz electromagnetic radiation at room temperature. The difference in the gate voltage dependences for 0.2 THz and 1.6 THz radiation and spatial pattern of the transistor response to focused 1.6 THz radiation confirms that the mechanism of detection is linked to the excitations of the two-dimensional electrons in the device channel.

(Some figures in this article are in colour only in the electronic version)

1. Introduction

n-channel or p-channel field effect transistors (FETs) can be used as fast room temperature detectors of THz radiation [1, 2]. The mechanism of the detection is based on the excitation of resonant or overdamped plasma waves in the device channel [3]. One of the important device parameters for optimizing the detection efficiency is the momentum relaxation time and thus indirectly the mobility of the charged carriers.

High mobility is offered by GaAs/AlGaAs [3–6], InGaP/InGaAs/GaAs [7], InGaAs/AlInAs [8] and AlGaIn/GaN HEMTs [4], in which detection of THz and sub-THz radiation has been measured. Si MOSFETs have also been shown to function as THz detectors [11–13]. These FET-type detectors can operate at room temperature, at high speed [1], and demonstrate a noise equivalent power (NEP) comparable to other room temperature detectors of terahertz radiation.

Si-based detectors, operating at room temperature, have an advantage of compatibility with mainstream CMOS technology, although the HEMT structures offer far higher mobility. Higher mobility can also be obtained from strained-Si technology. For instance, strained-Si modulation doped FETs with a Schottky gate contact show high mobility

and high operation speeds [14]. This enhanced electron mobility in the channel provides the potential to operate a FET as a plasmonic FET detector in the resonant mode with higher selectivity, higher responsivity and lower NEP. In [15], the first investigation of THz detection by strained-Si modulation doped FETs (MODFET) at low temperature (18 K) was presented. In this paper, we report on the behavior of a strained-Si MODFET as broadband detector at room temperature and as a function of the drain current.

2. Device and experimental set-up

The epistucture of the MODFET was grown by molecular beam epitaxy (MBE) on a thick relaxed SiGe virtual substrate grown by low-energy plasma-enhanced chemical vapor deposition (LEPECVD). The final Ge concentration in the virtual substrate was $x_{\text{Ge}} = 45\%$. The device had a 9 nm tensile strained (in terms of biaxial deformation) Si channel sandwiched between two heavily doped SiGe electron supply layers to generate a high carrier density in the strained-Si quantum well. The top of the device layers was capped with a thin layer of Si, so as not to compromise the quality of the Schottky gate. The ohmic contacts were not self-aligned. The transistors measured had a gate length of $L_g = 100$ nm, gate width $W = 30$ μm and source–drain distance of $L = 1$ μm .

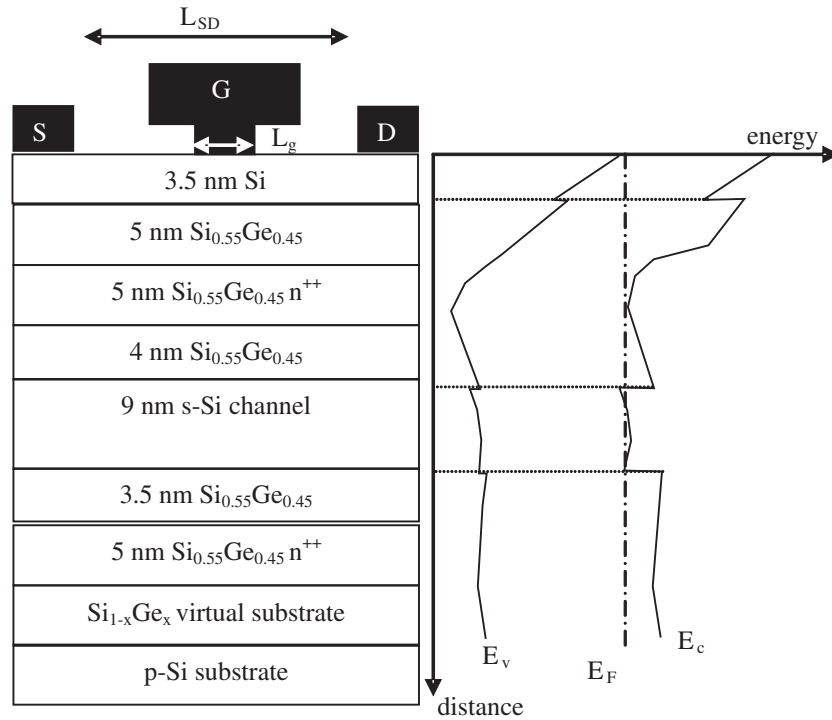


Figure 1. Left: schematic layer structure of the strained-Si modulation doped field effect transistors. Right: schematic energy band diagram calculated using MEDICITM.

Figure 1 shows the device layers and a schematic of the contacts together with the energy band diagram for the structure in the un-biased state. The strain in the Si layer caused formation of a quantum well for electrons and confinement of the carriers. The carrier concentration in the quantum well of $n_s = 4.6 \times 10^{12} \text{ cm}^{-2}$ and the mobility $\mu = 1355 \text{ cm}^2 \text{ V}^{-1} \text{ s}^{-1}$ were obtained by Hall measurements at room temperature. The conduction band offset can be estimated as $\Delta E_c = 0.6 \times x_{\text{Ge}} = 270 \text{ meV}$. The other effect of the strain is to split the conduction band degeneracy causing a lowering in energy of the Δ_2 bands. This has two consequences. First, the phonon scattering rate decreases, increasing the momentum relaxation time, and second, the effective mass, with which the electrons travel in the Δ_2 bands, decreases as well. The advantage of reduced phonon scattering in strained-Si channels disappears with decreasing temperatures (down to 100 K), when phonon scattering becomes less important. However, the decrease in effective mass remains important at lower temperatures [16]. The increased momentum relaxation time in tensile strained Si channels at room temperature promises to be advantageous for room temperature THz detection.

The response measurements were performed at 200 GHz using a 100 GHz Gunn diode and frequency doubler and at 1.6 THz with a CO₂ pumped FIR laser. The maximum output power was $\sim 3 \text{ mW}$ and $\sim 50 \text{ mW}$ for the 200 GHz and 1.6 THz systems, respectively. The radiation was focused on the transistor surface with a parabolic mirror. The sample holder was placed in the focal plane, on a computer-controlled nano-positioning stage.

No special coupling antennas were used in the experiment. The radiation was thus most likely coupled to the device via

the metallization pads. The radiation intensity was modulated by a mechanical chopper at 40–200 Hz. The source terminal of the device was grounded. A controlled DC drain current, I_d , was driven through the device using a Keithley Source Meter 2410. The gate bias was controlled by another Keithley Source Meter 2410. The current and gate voltage dependence of the response was measured using a voltage preamplifier ($\sim 8 \text{ M}\Omega$ input resistance) followed by a lock-in amplifier.

3. Measurements and discussion

Figure 2 shows the dc voltage induced on the drain (response) by the sub-terahertz radiation of $f = 0.2 \text{ THz}$ at different drain currents. As predicted by the theory [2, 17], the response increases with drain current.

For a radiation power of $\sim 1 \text{ mW}$, the responsivity is $R \approx 2 \text{ V W}^{-1}$ at zero drain current and reaches a relatively large value of approximately 55 V W^{-1} at $I_d = 1 \mu\text{A}$. The dimensions of the MODFET are smaller than the focus area of the incoming radiation beam and smaller than half the radiation wavelength, $\lambda/2$. Thus, only a fraction of the incoming radiation can be coupled into the MODFET. A method to increase responsivity is to combine several transistors in an array. Taking the area of the focused beam equal to $\lambda^2/4$ and a transistor area of $A_{\text{tr}} = 1.4 \times 10^{-4} \text{ cm}^2$, we estimate that, for a matrix of 6×6 transistors, a maximum responsivity might be as high as $R \approx 2000 \text{ V W}^{-1}$.

Figure 3 compares the normalized response of the MODFET to 0.2 THz and 1.6 THz radiation at a current $I_d = 0$. The absolute value of the maximum response at 1.6 THz was $\sim 0.1 \text{ mV}$. For a power at the focal plane

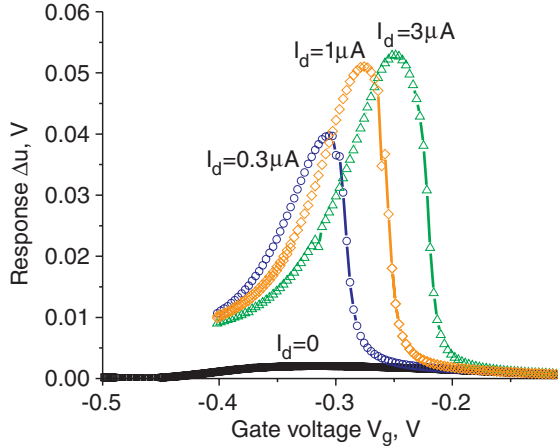


Figure 2. The dependence of the induced DC drain voltage on gate bias for different imposed drain currents for 0.2 THz radiation.

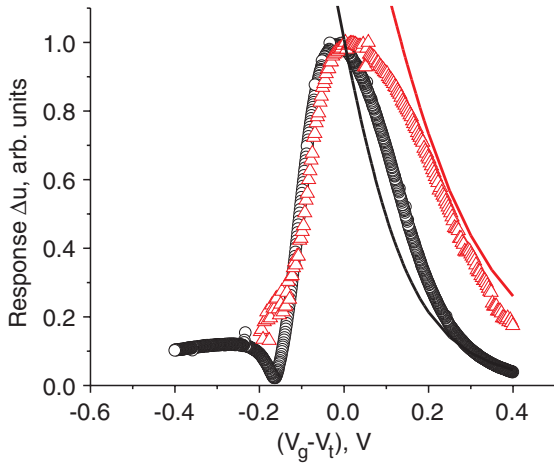


Figure 3. Response for 0.2 (circles) and 1.6 (triangles) THz radiation at a current $I_d = 0$ A. Lines are calculations using the model presented in [18]. The response is normalized to its maximum value.

of approximately 50 mW, the responsivity is $R \approx 2 \times 10^{-3} \text{ V W}^{-1}$.

As seen from figure 3, the response curve for the 0.2 THz radiation is narrower. The lines in figure 3 are the result of calculations as in [18],

$$\Delta u \propto \frac{1 \sinh^2 Q - \sin^2 Q}{s^2 \sinh^2 Q + \cos^2 Q}, \quad (1)$$

where

$$Q = \sqrt{\frac{\omega}{2\tau}} \frac{L}{s},$$

$$s^2 = s_0^2 \left(1 + \exp\left(-\frac{e(V_g - V_t)_0}{\eta k_B T}\right) \right) \times \ln \left(1 + \exp\left(\frac{e(V_g - V_t)}{\eta k_B T}\right) \right)$$

is the plasma wave velocity, $s_0 = \sqrt{\frac{\eta k_B T}{m}}$, η is the ideality factor. As seen, the theory describes the difference in the shape for the response to different frequencies qualitatively. The decrease of the response below threshold relates to the gate

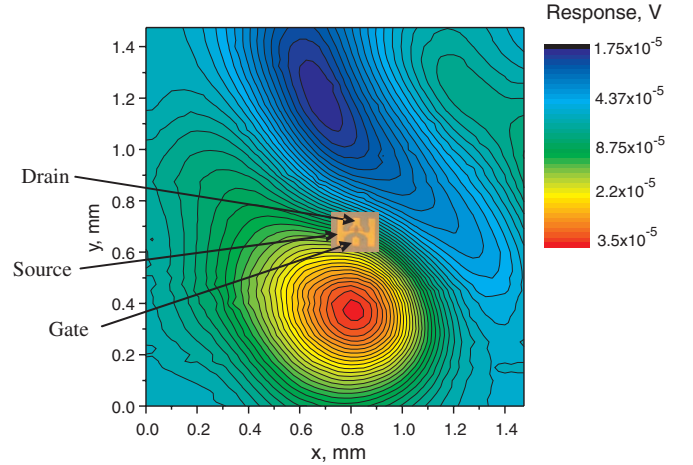


Figure 4. The responsivity pattern. $f = 1.6$ THz, $V_{gs} = -0.2$ V, $I_{ds} = 0$ A, $P \approx 50$ mW. The beam is focused by a parabolic mirror.

leakage current [18] and to the increased internal resistance of the detector caused by a large decrease of the electron density in the channel in the below threshold regime [13].

Figure 4 presents the measured 2D image of the transistor's terahertz responsivity versus its displacement in the focal plane of the incident beam. Polarization is parallel to the gate stripe. Two maxima, positive and negative, are located away from the transistor itself. The presence of a response of different sign has been reported earlier [19] and has been explained by the overdamped plasma wave excitations at the source and drain, respectively.

As seen from figure 4, the maximum values of both positive and negative signals occur when the beam focus is away from the transistor. This is the evidence of inefficient coupling of the THz radiation to the devices, and optimized coupling might lead to a large increase in the responsivity.

The theory [18] predicts the device responsivity should first increase with frequency and then saturate. In fact, the experimental data clearly show a much smaller response at 1.6 THz than at 200 GHz. One of the reasons is that the inductances of the bonding wires might effectively isolate the source and gate making the device look nearly symmetrical at high (1.6 THz) frequency and diminishing an asymmetry in the boundary conditions for the plasma waves excited at source and drain sides of the channel. That significantly reduces the response in comparison to the case of 200 GHz. In addition, the gate resistance, R_g , is enhanced by the skin effect. Skin layer thickness and its resistance are estimated to be $\delta = 60\text{--}70$ nm and $R_g = 50\text{--}100 \Omega$ at $f = 1.6$ THz. The time constant $\tau = R_g C_g$ is about one order of magnitude higher than the period $1/2\pi f$ (where C_g is the gate capacitance and $f = 1.6$ THz). This leads to the response decrease as $1/\omega^2$ or $1/\omega^3$ for the frequencies higher than $1/\tau$ when the skin layer thickness is higher or smaller than the gate metal thickness, respectively.

4. Conclusion

In conclusion, we demonstrated the detection of 0.2 THz and 1.6 THz radiation by the strained-Si modulation doped field

effect transistors at room temperature. The difference of the shape of the response versus gate voltage between 0.2 THz and 1.6 THz is explained based on the model of overdamped plasma waves in a 2D electron gas. The spatial variation of the transistor response to focused 1.6 THz radiation confirms the overdamped plasma waves mechanism of detection and holds promise for the responsivity increase with an optimized coupling structure.

Acknowledgments

K Fobelets acknowledges travel funding from EPSRC (EP/F044666/1). S L Rumyantsev acknowledges partial financial support provided by the RFBR (grant 08-02-00512-a). The work at RPI was partially supported by the ONR, by the NSF (under the auspices of CONNECTION ONE I/UCRC), and by the Institute for Nanoelectronics Discovery and Exploration (INDEX) supported by the Semiconductor Industry Association and the Semiconductor Research Corp.

References

- [1] Kachorovskii V Yu and Shur M S 2008 *Solid State Electron.* **52** 182
- [2] Stillman W and Shur M S 2007 *J. Nanoelectron. Optoelectron.* **2** 209
- [3] Dyakonov M and Shur M S 1993 *Phys. Rev. Lett.* **71** 2465
Dyakonov M and Shur M S 1996 *IEEE Trans. Electron Dev.* **43** 380
- [4] El Fatimy A *et al* 2006 *Electron. Lett.* **42** 1342
- [5] Knap W, Deng Y, Rumyantsev S, Lü J-Q, Shur M S, Saylor C A and Brunel L C 2002 *Appl. Phys. Lett.* **80** 3433
- [6] Lee M, Wanke M C and Reno J L 2004 *Appl. Phys. Lett.* **86** 033501
- [7] Peralta X G, Allen S J, Wanke M C, Harff N E, Simmons J A, Lilly M P, Reno J L, Burke P J and Eisenstein J P 2002 *Appl. Phys. Lett.* **81** 1627
- [8] Antonov A V *et al* 2004 *Phys. Solid State* **46** 146
- [9] Otsuji T, Hanabe M and Ogawara O 2004 *Appl. Phys. Lett.* **85** 2119
- [10] Knap W, Lusakowski J, Parenty T, Bollaert S, Cappy A, Popov V V and Shur M S 2004 *Appl. Phys. Lett.* **84** 2331
- [11] Knap W, Teppe F, Meziani Y, Dyakonova N, Lusakowski J, Buf F, Skotnicki T, Maude D, Rumyantsev S and Shur M S 2004 *Appl. Phys. Lett.* **85** 675
- [12] Tauk R *et al* 2006 *Appl. Phys. Lett.* **89** 252511
- [13] Stillman W, Shur M S, Rumyantsev S, Veksler D and Guarin F 2007 *Electron. Lett.* **43** 422
- [14] Aniel F *et al* 2003 *Solid-State Electron.* **47** 283
- [15] Richard S, Zerounian N, Boucaud P, Ortega J M, Hackbarth T, Herzog H J and Aniel F 2005 *Proc. ESSDERC 2005: 35th European Solid-State Dev. Research Conf.* p 363
- [16] Fobelets K, Gaspari V and Velasquez-Perez J E 2007 Origin of performance improvement of sub-micron strained-Si MOSFETs compared to Si MOSFETs as a function of temperature *Internal Report* Imperial College London
- [17] Veksler D, Teppe F, Dmitriev A P, Kachorovskii V Yu, Knap W and Shur M S 2006 *Phys. Rev. B* **73** 125328
- [18] Knap W *et al* 2002 *J. Appl. Phys.* **91** 9346
- [19] Veksler D B, Muraviev A V, Elkhatib T A, Salama K N and Shur M S 2007 *Proc. ISDRS 2007, Int. Semiconductor Device Research Symp.* (12–14 Dec. 2004)